

Tramadol Causes Weight, Nissl Substance, and Astrocytic Changes in the Hippocampal Formation's Structures

Ubong Udeme Ekpo ^{1*}, James Onah Ikpa ^{1,2}, Bethel Onyinoyi Onimisi ³,
Joy Ochai ^{1,4}, Oderinde Peter Gbenga ¹

¹Department of Human Anatomy,
Ahmadu Bello University (ABU),
Zaria,
Nigeria.

²Department of Human Anatomy,
University of Cross River State,
Cross River State.

³Department of Anatomy,
Usman Danfodiyo University, Sokoto,
Nigeria.

⁴Department of Human Anatomy,
Federal University of Health Sciences,
Otukpo,
Benue State.

Email: ubongekpo023@gmail.com

Abstract

Tramadol hydrochloride is a centrally acting synthetic opioid which is used to treat moderate to moderately severe pain and is reported to have neurotoxic potential. Therefore, this study investigated the effects of tramadol on weight, Nissl bodies and astrocytic changes in the structures of the hippocampal formation. 2ml/kg of distilled water was given to the control group and 50mg/kg tramadol to group 2 orally for 21 days. The weight of the rats was taken before and after the experiment. The rats were euthanized, brains harvested and weighed. The harvested brains were fixed in 10% formal saline, and processed routinely, stained with Cresyl fast violet (CFV) for demonstration of Nissl substance and glial fibrillary acidic protein (GFAP) for demonstration of astrocytes expression. CFV stain revealed a reduced staining intensity of these regions with pathological changes in the tramadol-treated group. GFAP showed numerous reactive astrocyte processes; overlapping and interdigitation of astrocyte processes; astrocyte proliferation; astrocyte cell body hypertrophy and thickening of astrocyte processes. This study's findings revealed changes in weight, Nissl bodies and hippocampal formation histopathology.

Keywords: hippocampal formation, histochemistry, histopathology, immunohistochemistry, neurodegeneration

INTRODUCTION

Opioid abuse has emerged as a global health crisis, affecting individuals of diverse backgrounds and communities worldwide. Among the opioids, tramadol has gained

increasing attention due to its unique pharmacological profile and its potential for abuse. Tramadol, a synthetic opioid analgesic, acts as a mu-opioid receptor agonist and exerts additional effects on the noradrenergic and serotonergic systems, distinguishing it from traditional opioids (Toufique, 2022). Tramadol primarily acts on the mu-opioid receptors, inhibiting the reuptake of norepinephrine and serotonin, thereby modulating pain perception and transmission (Dayer *et al.*, 1997). This dual mechanism of action contributes to its analgesic efficacy, making it widely prescribed for the management of moderate to severe pain, including postoperative, dental, and chronic pain conditions (Wiffen *et al.*, 2014). Tramadol abuse has become a significant concern on a global scale, with reports of its misuse and diversion increasing in various regions. In Africa, tramadol abuse has reached alarming levels, with several countries experiencing a surge in its illicit use (United Nations Office on Drugs and Crime, 2019). Nigeria, in particular, has witnessed a notable rise in tramadol abuse, with the drug gaining popularity among diverse populations. Factors contributing to its widespread abuse include its easy accessibility, low cost, misconceptions about its safety, and limited regulatory control (Akunna & Lucyann, 2023). The abuse of tramadol can have profound effects on the brain. Chronic misuse of tramadol has been associated with alterations in the brain's reward circuitry, neuroplasticity, and neurotransmitter systems (Karila *et al.*, 2008). Moreover, excessive tramadol use has been linked to the development of physical dependence, tolerance, and withdrawal symptoms (Messer *et al.*, 2017).

The hippocampal formation is a critical brain region involved in various cognitive processes, including learning, memory formation, and spatial navigation (Eichenbaum, 2017). It comprises several interconnected structures, including the hippocampus proper (dentate gyrus, CA1, CA2, and CA3 subfields) and the entorhinal cortex (Fanselow & Dong, 2010). Opioids, a class of drugs commonly used for pain relief, can have profound effects on the hippocampal formation and its constituent structures (Dinis-Oliveira, 2019). Opioid receptors are present in various regions of the hippocampal formation, including the dentate gyrus, CA1, CA3, and CA4 regions. Activation of these receptors by opioids can modulate neuronal activity and neurotransmitter release (Nam *et al.*, 2021). Opioids have been shown to affect synaptic plasticity, a cellular process underlying learning and memory. Chronic opioid exposure can impair long-term potentiation (LTP), a form of synaptic plasticity associated with memory formation, in the hippocampus (Heinsbroek *et al.*, 2021). Studies have demonstrated that chronic opioid use can lead to cognitive impairments, including deficits in spatial learning and memory. These effects may be mediated by alterations in the hippocampal formation (Schoenbaum *et al.*, 2006). Opioids have been found to influence hippocampal neurogenesis, the process of generating new neurons in the adult brain. Prolonged opioid exposure can reduce neurogenesis in the dentate gyrus, potentially contributing to cognitive dysfunction (Eisch *et al.*, 2000). Opioids have been associated with neuroinflammatory responses in the hippocampal formation. Increased activation of microglia, the immune cells of the brain, and elevated pro-inflammatory cytokines have been observed following opioid administration (Hutchinson *et al.*, 2011).

Despite the fact that studies have examined the neurotoxic effects of tramadol on several areas of the brain. As far as we are aware, tramadol's neurotoxic on the structures of the hippocampal formation are unknown. Moreover, the present study aims to address the knowledge gap and contribute to existing information on the potential mechanisms of tramadol brain damage, with the goal of informing the design of more effective therapeutic interventions. Thus, the need for this study.

MATERIALS AND METHODS

Ethical approval

This study's ethical approval was granted by the Ahmadu Bello University Ethics Committee on Animal Use and Care, with approval code ABUCAUC/2022/031.

Experimental animals

Prior to studies, twelve adults male Wistar rats were obtained from the Animal House of the Faculty of Pharmaceutical Sciences at Ahmadu Bello University and housed in wired cages for a period of two weeks. They had unlimited access to water and pelletized feed.

Purchase of drug and chemical

Tramadol hydrochloride (50 mg capsules), produced by VADIS PHARM. LTD. Plot RD-14-Trans-Ekulu, Enugu, Nigeria was procured and used for the study. Ketamine (50 mg/ml ketamine hydrochloride injection USP) was utilized as the anesthetic. It was procured from Swiss Parenterals PVT Ltd. In Gussjarat, India.

Drugs administration

The dosage of the medications was estimated based on the weight of the animals and administered. It was suspended in a normal saline solution and freshly given to the rats by feeding them through a needle.

Experimental design and treatment of animals

A total of twelve (12) male Wistar rats were allocated into two groups of six (6) each at random. Control group (2 ml/kg of water) and tramadol-treated group (50 mg/kg) (Ekpo *et al.*, 2023). Every administration was carried out orally, once every day for 21 days.

Morphological Studies

The body weight of the rats was taken at the beginning and at the end of the experiment. After the experiment, the data were analyzed for body weight changes. The brain weight was measured immediately after dissection and was used in determining the organ-weight index

Animal Euthanization

After completion of the experiment, the animals were anesthetized with 75 mg/kg ketamine intraperitoneally (Kurdi *et al.*, 2014), and perfused transcardiacally with normal saline and 10 % formol saline. The rats' brains were carefully removed from their skulls after perfusion and cleaned with normal saline. The skull was opened at the midline, and the brains were removed and preserved for 48 hours in 10 percent formalin. The fixed brains were taken to the Histology Unit, Department of Human Anatomy, Ahmadu Bello University, Zaria, for tissue processing and staining.

Visualization of Nissl substance by Cresyl Fast Violet stain

The Carson technique (Carson, 1997) was used. Brain tissues from the hippocampal region were deparaffinized and dried in distilled water. The slides were rapidly rinsed in one change of distilled water after being incubated in Cresyl Violet Stain Solution (0.1 percent) for 2 minutes. Following a brief dehydration in absolute alcohol, the sections were rapidly cleaned in xylene, mounted in synthetic resin, and cover slipped with DPX mountant.

Glial Fibrillary Protein (GFAP) Analysis

This work used the modified avidin-biotin-peroxidase complex (ABC) method of Hsu *et al.* (1981), according to Yoshida *et al.* 1990. 5 m thick sections of the brain were fixed for 6 hours

in 10 % phosphate-buffered formalin. Endogenous peroxidase was blocked before the primary antibody, 1/100 anti-GFAP (Abcam, UK), was applied to the sections. The section was then treated with Mouse/Rabbit HRP (BioSB, Spain) for 45 minutes. The immunostained slices were dried, cleaned, and mounted in DPX after being mildly counterstained for 1 minute with Mayer and Haematoxylin (Dako, Glostrup, Denmark). The primary antibody was taken out and non-immune serum was utilized to carry out the control sections for the IHC of GFAP.

Quantification of Nissl Substance Distribution

Nissl substance quantification of neuronal cells was measured by the quantification of Nissl substance reactivity to Creyls Fast Violet, an excellent neuronal (cell body-specific) stain which is useful for the demonstration of Nissl substance in neurons (Suvarna *et al.*, 2011; Ekpo *et al.*, 2023). The manufacturer's instructions were followed for measuring the staining intensity from the Creyls Fast Violet-stained micrographs (digital micrograph imaging) using a computer running image analysis software (Image J, NIH, US) (Eluwa *et al.*, 2013). To reduce bias values brought on by different image quality, the Image J region of interest (ROI) manager tool for examination of specific sections of the micrographs was used. (*Image acquisition setting and exposure time*) (Amber *et al.*, 2020).

Data Analysis

Data were shown as mean and SEM (standard error of the mean). Student t-test was employed to see the mean difference between the groups and two-way split ANOVA for differences within the groups. Statistically significant values were those with $P < 0.05$. Data analysis was done using statistical product and service solutions (IBM SPSS 26).

RESULTS

Body weight estimation

The body weights of the rats before and after the experiments were observed. There was a significant increase ($p < 0.05$) when the initial body weight was compared to the final body weight in the control and the tramadol group (Fig 1A). There was no significant ($p > 0.05$) difference in the final body weight, and a percentage weight change in the tramadol treated group when compared to the control (Fig 1B).

Brain weight estimation

There was no ($p > 0.05$) statistical increase or decrease in brain weight (Fig 1C) and brain body weight index (BBWI) when compared to the control (Fig 1D).

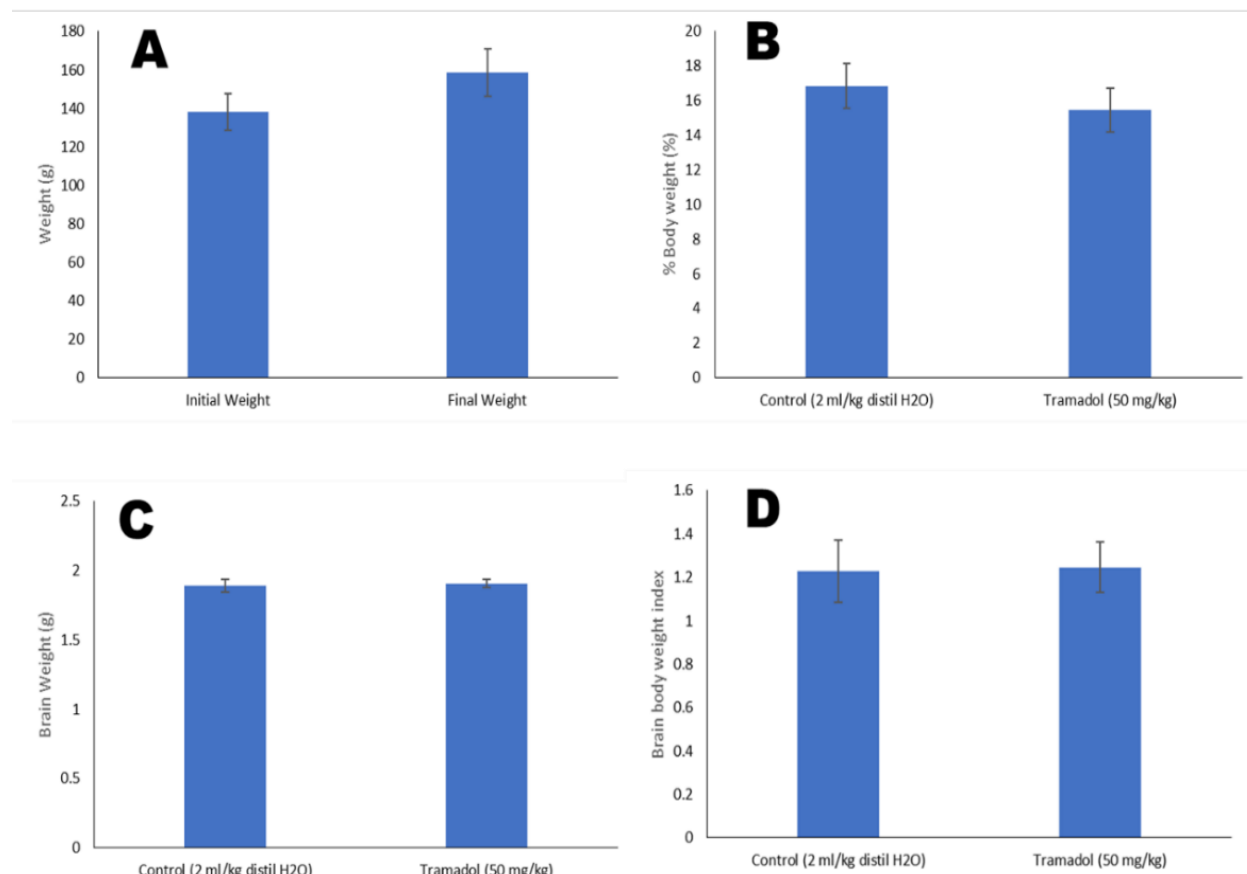


Figure 1: (A) Body weight of Wistar rats following oral administration of tramadol. (B) Percentage body weight of Wistar rats following oral administration of tramadol. (C) Brain weight of Wistar rats following oral administration of tramadol. (D) Brain body weight change of Wistar rats following oral administration of tramadol. n=6; mean \pm SEM, Student *t*-test. *Tukey post-hoc test*, $*=p<0.05$ when tramadol group was compared to control group.

Expression of Nissl substance using Cresyl Fast Violet stain (CFV)

Effects of tramadol on the entorhinal cortex

Histochemical examination of the coronal section of the entorhinal cortex reveals neuronal cells arranged in layers I, II, III, IV, V, and VI. The control group shows intensely stained layer I, which is poorly cellular, layer II, which contains islands of rounded cells with nuclei having prominent nucleoli (arrows), and III, which contains medium pyramidal cells with prominent nucleoli in their nuclei, layer IV pointing to lamina dissecans with small pyramidal cells and stellate cells, layer V containing mainly large pyramidal cells, and layer VI containing cells of various sizes and shapes. The tramadol-treated group showed reduced staining intensity in layers I, II, III, IV, V, and VI with neurodegenerative changes presenting as a pyknotic cell, dark neurons, chromatolysis, and karyolysis (Fig 2, 3 & 8).

Effects of tramadol on the dentate gyrus

The control group shows a normal appearance of the distinct intensely stained molecular layer, granular cell layer, and polymorphic layer of the dentate gyrus with normal pyramidal cells. The tramadol-treated group reveals the reduced staining intensity of the molecular layer, granular cell layer, and polymorphic layer of the dentate gyrus with neuronal degenerative change such as chromatolysis (Fig 4 & 8).

Effects of tramadol on the CA1 and CA3 regions

The control group shows intensely stained CA1 and CA3 regions that contain normal pyramidal cells while the tramadol-treated group shows the reduced staining intensity of CA1 and CA3 with degenerated neuronal cells such as chromatolysis, karyolysis, and vacuolation (Fig 5, 6 & 8).

Effects of tramadol on the subiculum

The control group reveals a normal appearance of the distinct intensely stained molecular layer, granular cell layer, and polymorphic layer of the subiculum with normal pyramidal cells while the tramadol-treated group shows a reduced staining intensity of the molecular layer, granular cell layer, and polymorphic layer of the subiculum with neurodegenerative changes such as chromatolysis and karyolysis (Fig 7 & 8).

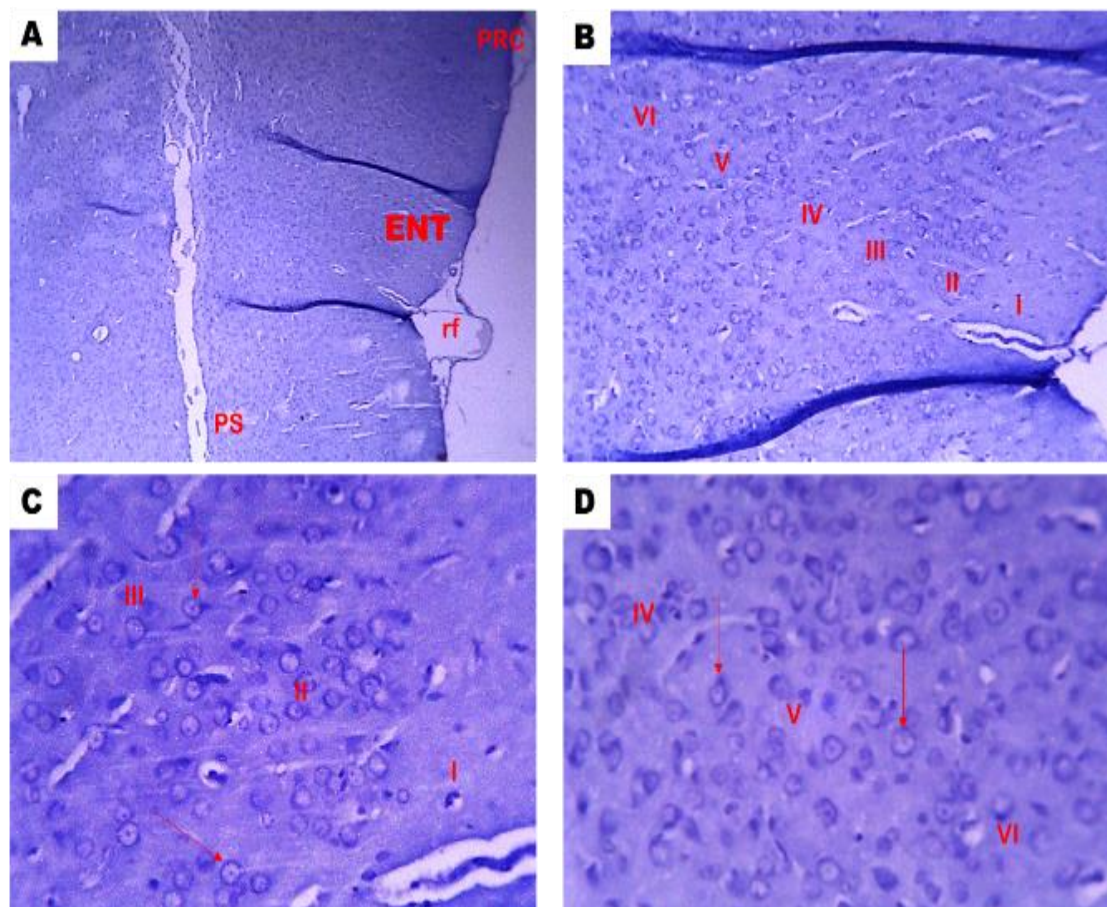


Figure 2: Photomicrographs of the entorhinal cortex (ENT) region. (A) Coronal section of adult Wistar rat cerebral hemisphere of control group showing the location of the entorhinal cortex, bounded medially by the parasubiculum (PS) and laterally by perirhinal cortex (PRC). Creyls Fast Violet stain, x 40. (B) Coronal section of the entorhinal cortex of control group showing neuronal cells arranged in layers I, II, III, IV, V, VI and rhinal fissure (rf). Creyls Fast Violet stain, x 100. (C) Section of the entorhinal cortex of the control group showing intensely stained layer I, which is poorly cellular, layer II, which contains islands of rounded cells with nuclei having prominent nucleoli (arrows), and III, which contains medium pyramidal cells with prominent nucleoli in their nuclei. Creyls Fast Violet stain, x 250. (D) Section of the entorhinal cortex of the control group showing intensely stained layer IV pointing to lamina dissecans, layer V containing mainly large pyramidal cells (arrow), and layer VI containing cells of various sizes and shapes. Creyls Fast Violet stain, x 250.

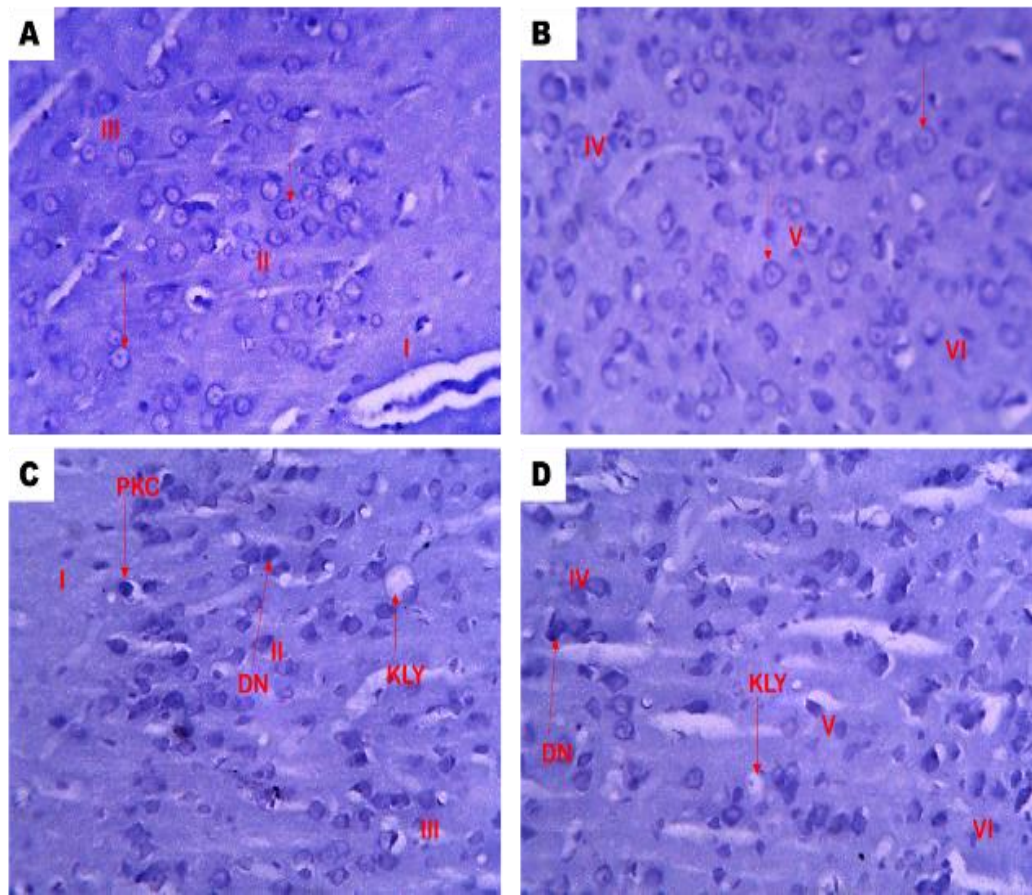


Figure 3: Photomicrographs of the entorhinal cortex (ENT) region. (A) Section of the entorhinal cortex of the control group showing layer I which is poorly cellular, layer II which contains islands of rounded cells with nuclei having large nucleoli (arrows), III which contains medium pyramidal cells with large nucleoli in their nuclei. Creyls Fast Violet stain, x 250. (B) Section of the control group's entorhinal cortex showing layer IV pointing to lamina dissecans, layer V containing mainly large pyramidal cells (arrows), and layer VI containing cells that have various sizes and shapes. Creyls Fast Violet stain, x 250. (C) Section of the entorhinal cortex of the tramadol-treated group showing reduced staining intensity in layers I, II, and III with neurodegenerative changes presenting as a pyknotic cell (PKC), dark neurons (DN), and karyolysis (KLY). Creyls Fast Violet stain, x 250. (D) Section of the entorhinal cortex of the tramadol-treated group showing reduced staining intensity in layers IV, V, and VI with degenerated neuronal cells presenting as dark neurons (DN) and chromatolysis (CLY). Creyls Fast Violet stain, x 250.

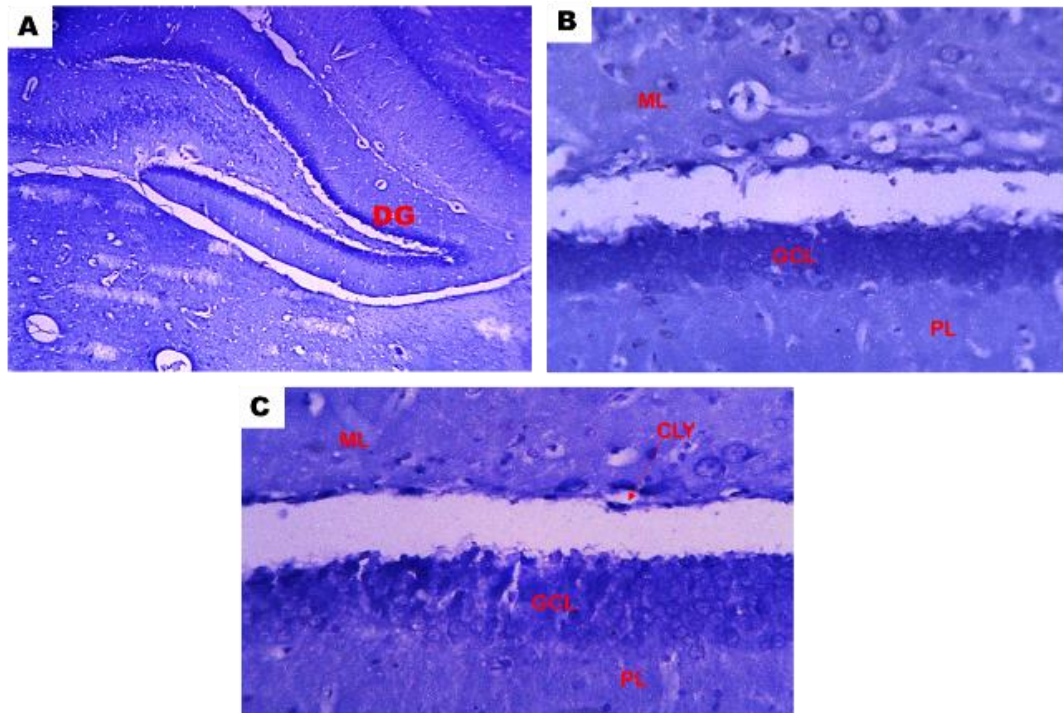


Figure 4: Photomicrographs of Wistar rat dentate gyrus (DG). (A) The control group showing the location of the dentate gyrus. Creyls Fast Violet stain, x 40. (B) The control group showing a normal appearance of the distinct intensely stained molecular layer (ML), granular cell layer (GCL), and polymorphic layer (PL) of the dentate gyrus with normal pyramidal cells (arrows). Creyls Fast Violet stain, x 250. (C) The tramadol-treated group showing the reduced staining intensity of the molecular layer (ML), granular cell layer (GCL), and polymorphic layer (PL) of the dentate gyrus with neuronal degenerative change such as chromatolysis. Creyls Fast Violet stain, x 250.

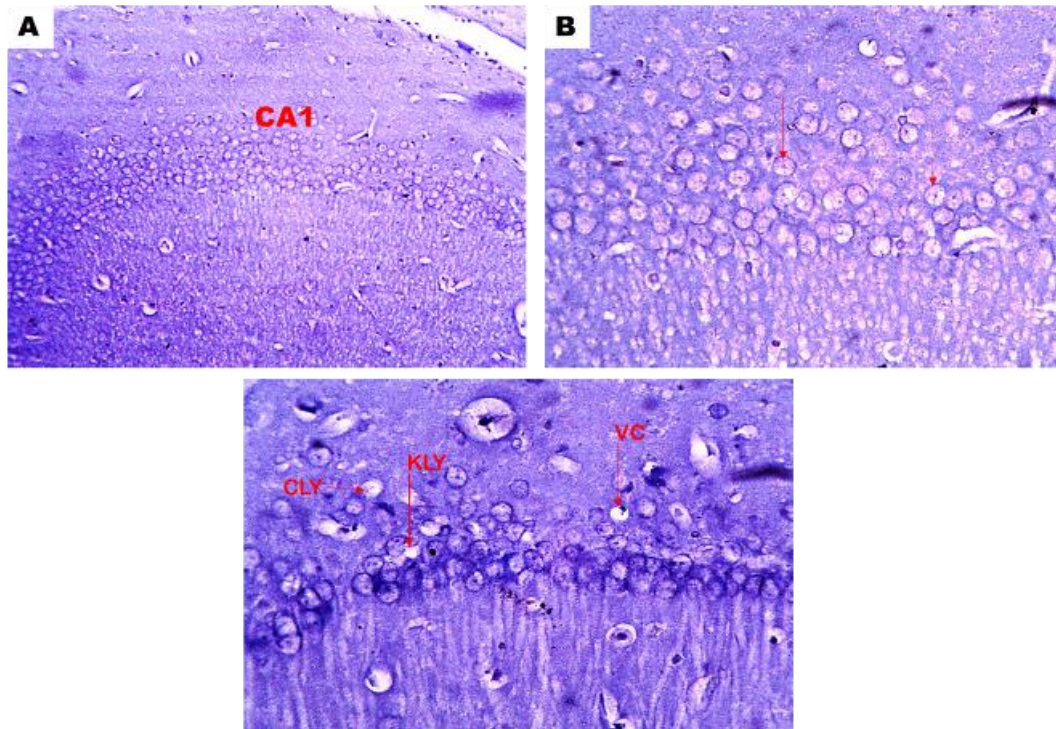


Figure 5: Photomicrographs of the CA1 region of the hippocampus. (A) Section of Wistar rat hippocampal region of control group showing the location of CA1. Creyls Fast Violet stain, x 100. (B) Section of CA1 region of control group showing intensely stained CA1 containing normal pyramidal cells. Creyls Fast Violet stain, x 250. (C) Section of CA1 region of tramadol-treated group showing the reduced staining intensity of CA1 with degenerated neuronal cells such as chromatolysis (CLY), karyolysis (KLY), and vacuolation (VC). Creyls Fast Violet stain, x 250.

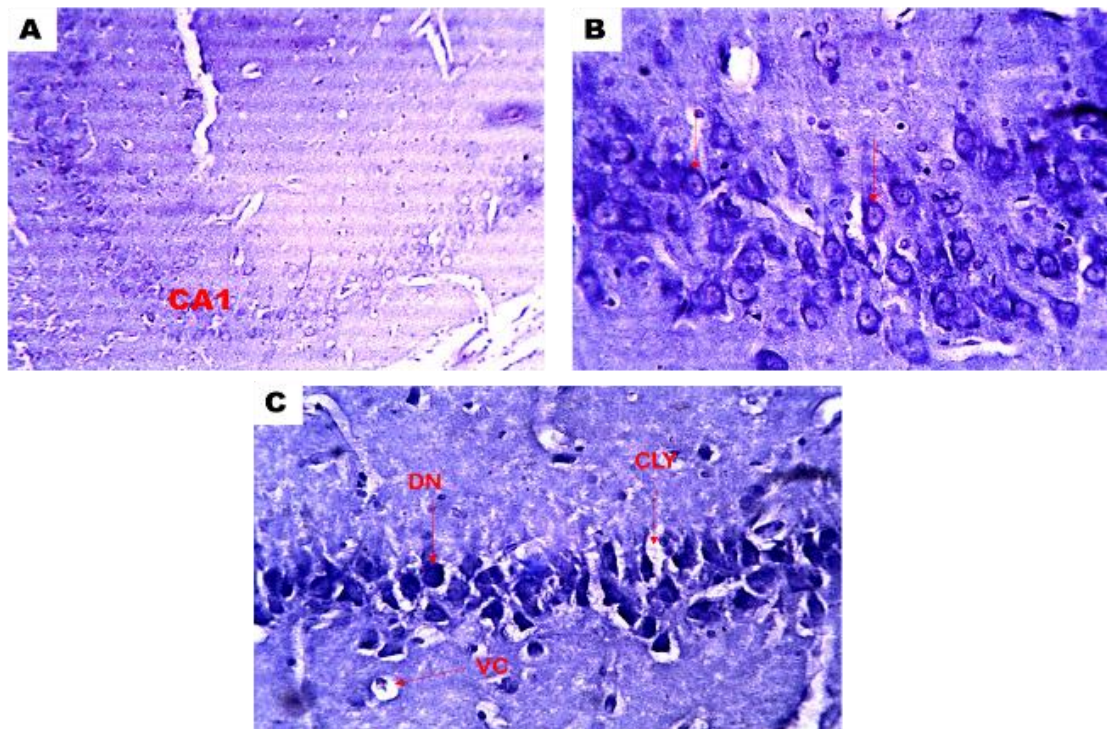


Figure 6: Photomicrographs of the CA3 region of the hippocampus. (A) Section of Wistar rat hippocampal region of control group showing the location of CA3. Creyls Fast Violet stain, x 100. (B) Section of CA3 region of control group showing intensely stained CA3 containing normal pyramidal cells (arrow). Creyls Fast Violet stain, x 250. (C) Section of CA3 region of tramadol treated group showing the reduced staining intensity of CA3 with degenerated neuronal cells such as chromatolysis (CLY), karyolysis (KLY), and vacuolation (VC). Creyls Fast Violet stain, x 250.

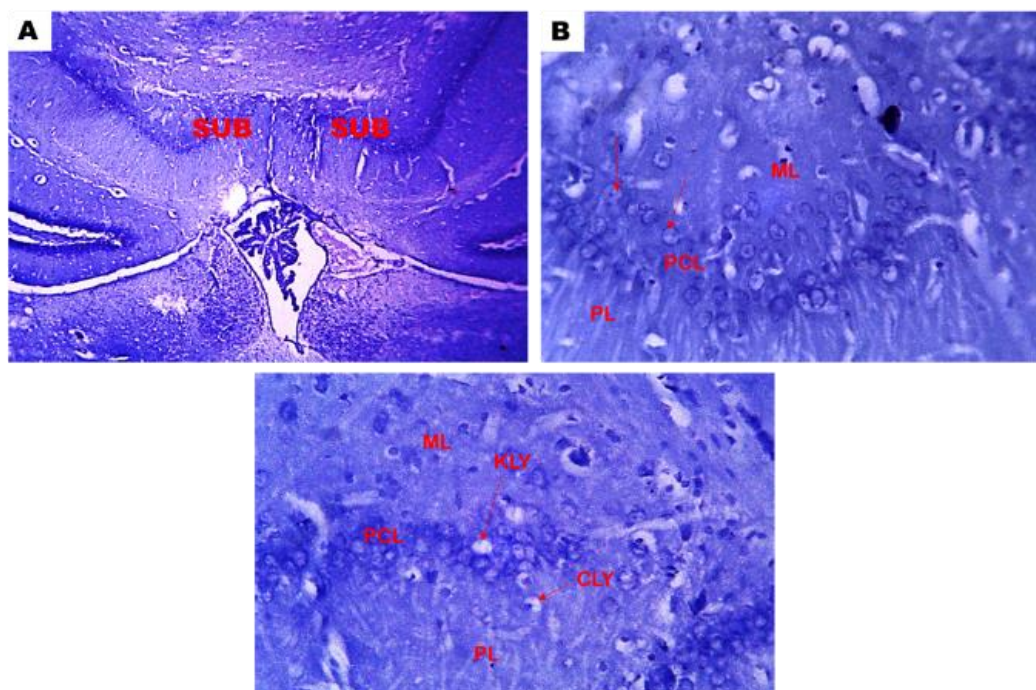


Figure 7: Photomicrographs of Wistar rat subiculum (SUB). (A) The control group showing the location of the subiculum. Creyls Fast Violet stain, x 40. (B) The control group showing a normal appearance of the distinct intensely stained molecular layer (ML), granular cell layer (PCL), and polymorphic layer (PL) of the subiculum with normal pyramidal cells. Creyls Fast Violet stain, x 250. (C) The tramadol group showing the reduced staining intensity of the molecular layer (ML), granular cell layer (GCL), and polymorphic layer (PL) of the subiculum with neurodegenerative changes such as chromatolysis (CLY) and karyolysis (KLY). Creyls Fast Violet stain, x 250.

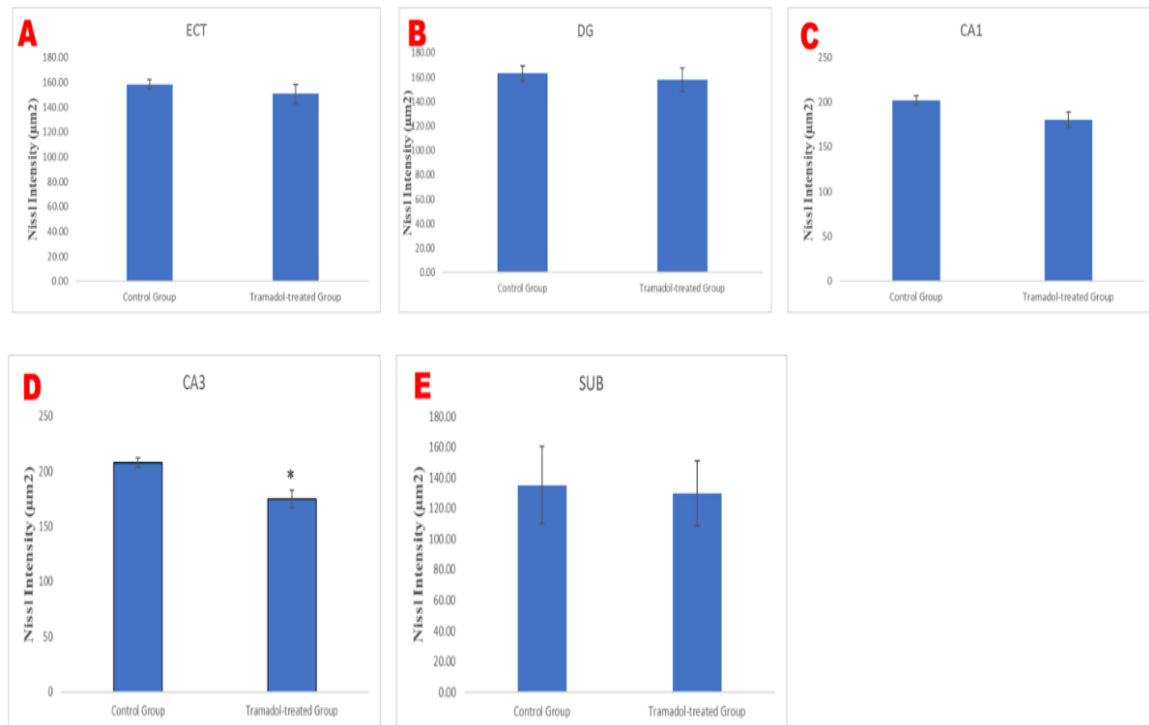


Figure 8: Measurement of staining intensity of sections of Wistar rats following oral administration of tramadol. n=6; mean ± SEM, student t-test, Tukey post-hoc test, $*=p<0.05$ when compared to control. Control = 2 ml/kg of distilled water, Tramadol-treated group = 50 mg/kg, ECT = entorhinal cortex, DG = dentate gyrus, CA1 = cornu ammonis, CA3 = cornu amonis, SUB = subiculum (A, B, C, D & E)

Astrocytic expression using Glial fibrillary acidic protein stain

There was a significant increase ($P\geq 0.05$) in the area of astrocytic expression in the entorhinal cortex, dentate gyrus, CA1, CA3, and the subiculum (Fig 15).

Effects of tramadol on the entorhinal cortex

The control group shows layers I, II, III, IV, and VI with few expressions of detectable levels of astrocytes with the astrocytes processes not overlapping (Figure 9 & 10) while the tramadol-treated group shows layers I & II with few expressions of detectable levels of astrocytes; layers III, IV, V & VI with moderate hypertrophy of the cell body of astrocytes with no overlapping of the processes (Fig 11).

Effects of tramadol on the dentate gyrus

The control group reveals a molecular layer, granular cell layer, and polymorphic layer with few expressions of detectable levels of astrocytes with no overlapping of astrocytes processes. The tramadol-treated group shows numerous reactive astrocyte processes; extensive overlapping and interdigitation of astrocyte processes; astrocyte proliferation and astrocyte cell body hypertrophy especially in the molecular layer (Fig 12).

Effects of tramadol on the CA1 and CA3 regions

The control group of CA1 and CA3 regions reveals few expressions of detectable levels of astrocytes with the astrocytes processes not overlapping. The tramadol-treated group of CA1 and CA3 regions has numerous reactive astrocytes processes; extensive overlapping and interdigitation of astrocytes processes; astrocytes proliferation; astrocytes cell body hypertrophy and thickening of astrocytes processes (Fig 13).

Effects of tramadol on the subiculum

The control group shows a molecular layer, pyramidal cell layer, and polymorphic layer with few expressions of detectable levels of astrocytes with no overlapping of astrocytes processes. The tramadol-treated group reveals numerous reactive astrocyte processes; extensive overlapping and interdigitation of astrocyte processes; astrocyte proliferation; astrocyte cell body hypertrophy and

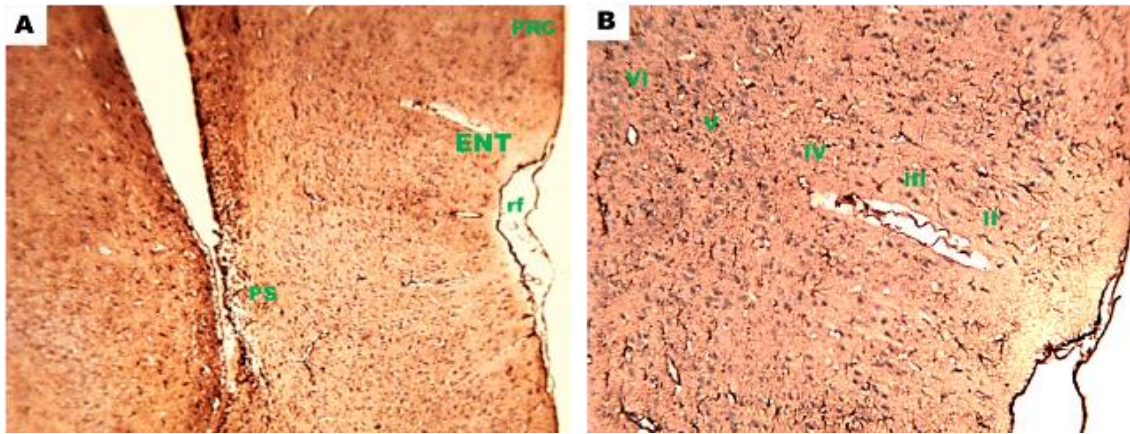


Figure 9: Photomicrographs of the entorhinal cortex (ENT) region. (A) Coronal section of adult Wistar rat cerebral hemisphere of the control group showing the location of the entorhinal cortex, bounded medially by the parasubiculum (PS) and laterally by perirhinal cortex (PRC). GFAP stain, x 40. (B) Coronal section of the entorhinal cortex of the control group showing layers I, II, III, IV, V, VI and rhinal fissure (RF). GFAP stain, x 100.

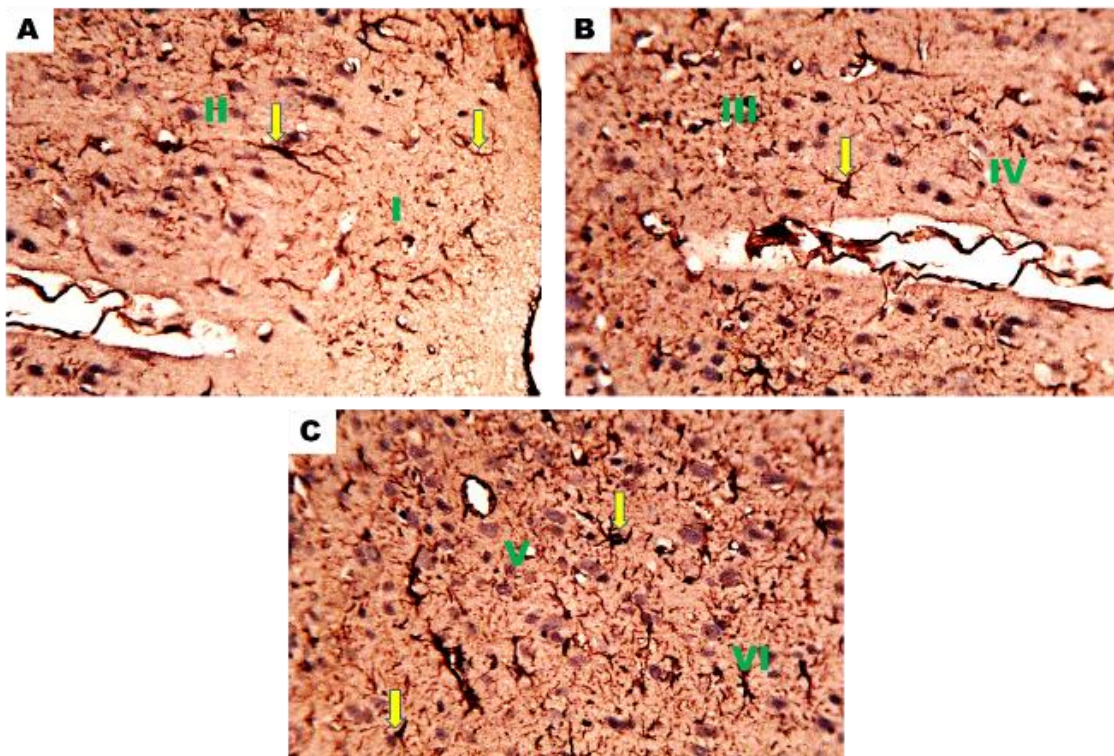


Figure 10: Coronal section of adult Wistar rat entorhinal cortex of the control group showing layers I, II, III, IV, and VI with few expressions of detectable levels of astrocytes (arrows); no overlapping of astrocytes processes. GFAP stain, x 250. (A, B & C).

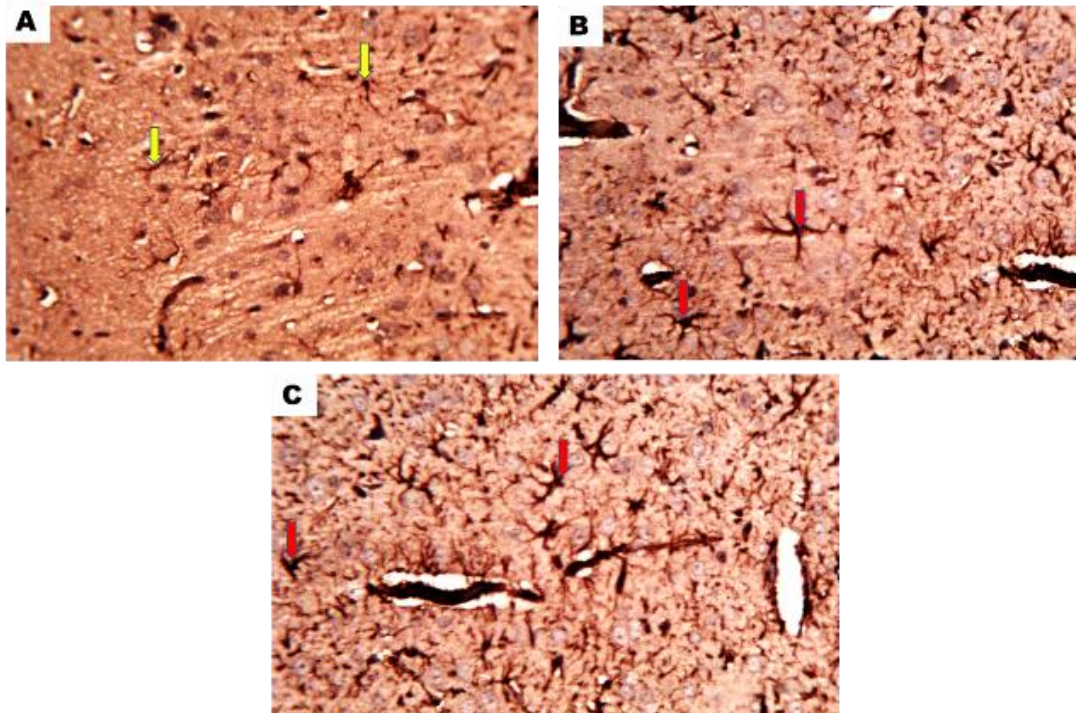


Figure 11: Coronal section of adult Wistar rat entorhinal cortex of the tramadol-treated group (A) Showing layers I & II with few expressions of detectable levels of astrocytes (arrows). GFAP stain, x 250. (B) Showing layers III & IV with moderate hypertrophy of the cell body of astrocytes with no overlapping of the processes. GFAP stain, x 250. (C) Showing layers V & VI with moderate hypertrophy of the cell body of astrocytes with no overlapping of the processes. GFAP stain, x 250.

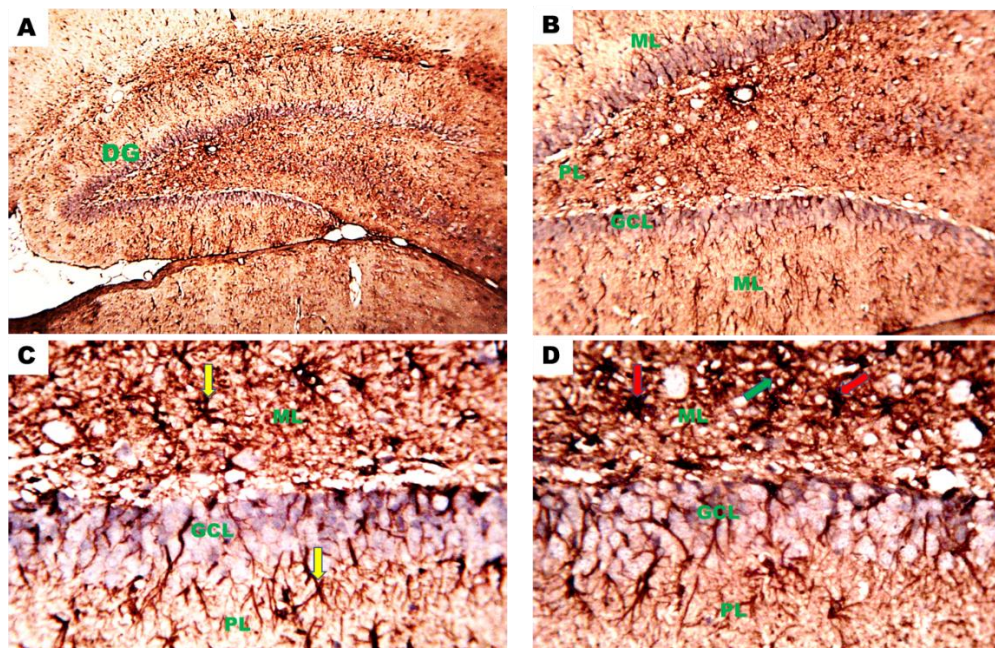


Figure 12: Photomicrographs of the dentate gyrus (DG) region. (A) The control group showing the location of the dentate gyrus (DG). GFAP stain, x 40. (B) The control group having three layers: the molecular layer (ML), the granular cell layer (GCL), and the polymorphic layer (PL). GFAP stain, x 100. (C) The control group showing molecular layer (ML), granular cell layer (GCL), and polymorphic layer (PL) with few expressions of detectable levels of astrocytes (arrows); no overlapping of astrocytes processes. GFAP stain, x 250. (D) The tramadol-treated group showing numerous reactive astrocytes processes; extensive overlapping and interdigitation of astrocytes processes (green arrows); astrocytes proliferation; astrocytes cell body hypertrophy (red arrows) especially in the molecular layer (ML). GFAP stain, x 250.

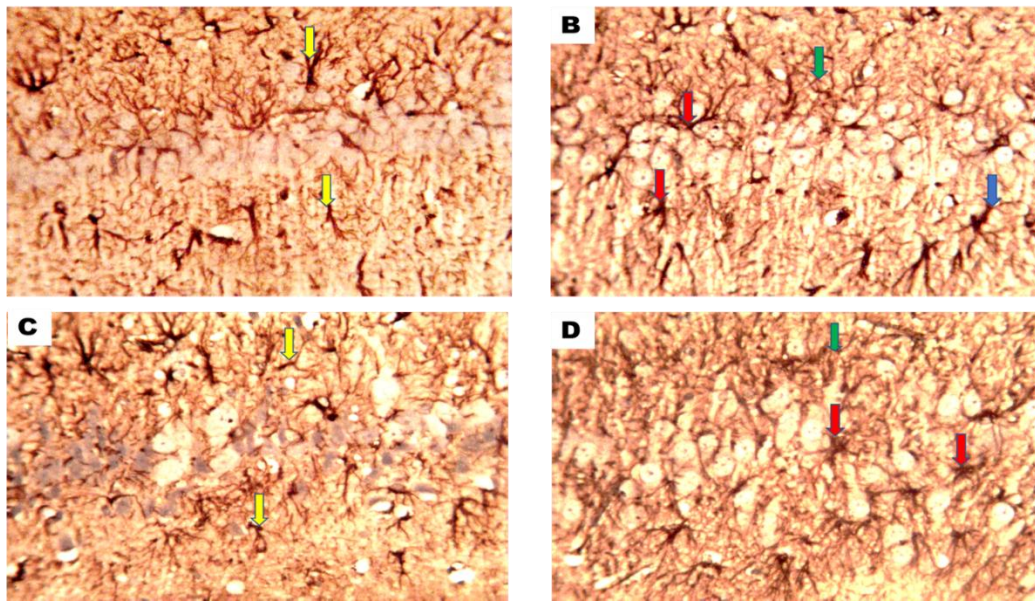


Figure 13: Photomicrographs of the CA1 & CA3 region of the hippocampus. (A) The control group showing few expressions of detectable levels of astrocytes (arrows); no overlapping of astrocytes processes. GFAP stain, x 250. (B) The tramadol-treated group having numerous reactive astrocytes processes; extensive overlapping and interdigitation of astrocytes processes (green arrows); astrocytes proliferation; astrocytes cell body hypertrophy (red arrows); thickening of astrocytes processes (blue arrows). GFAP stain, x 250. (C) The control group showing few expressions of detectable levels of astrocytes (arrows); no overlapping of astrocytes processes. GFAP stain, x 250. (D) The tramadol-treated group having numerous reactive astrocytes processes; extensive overlapping and interdigitation of astrocytes processes (green arrows); astrocytes proliferation; astrocytes cell body hypertrophy (red arrows). GFAP stain, x 250.

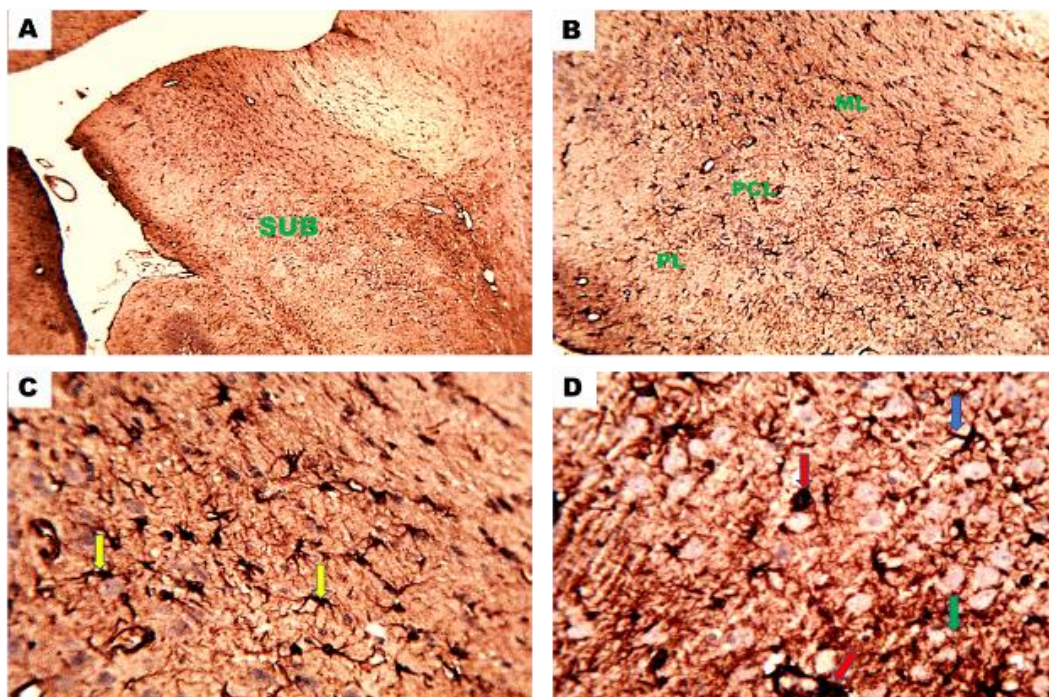


Figure 14: Photomicrographs of the subiculum (SUB) region. (A) The control group showing the location of the subiculum (SUB) region. GFAP stain, x 40. (B) The control group having three layers: the molecular layer (ML), the pyramidal cell layer (PCL), and the polymorphic layer (PL). GFAP stain, x 100. (C) The control group showing molecular layer (ML), pyramidal cell layer (PCL), and polymorphic layer (PL) with few expressions of detectable levels of astrocytes (arrows); no overlapping of astrocytes processes. GFAP stain, x 250. (D) The tramadol-treated group showing numerous reactive astrocytes processes; extensive overlapping and interdigitation of astrocytes processes (green arrows); astrocytes proliferation; astrocytes cell body hypertrophy (red arrows); increased thickening of astrocytes processes (blue arrow). GFAP stain, x 250).

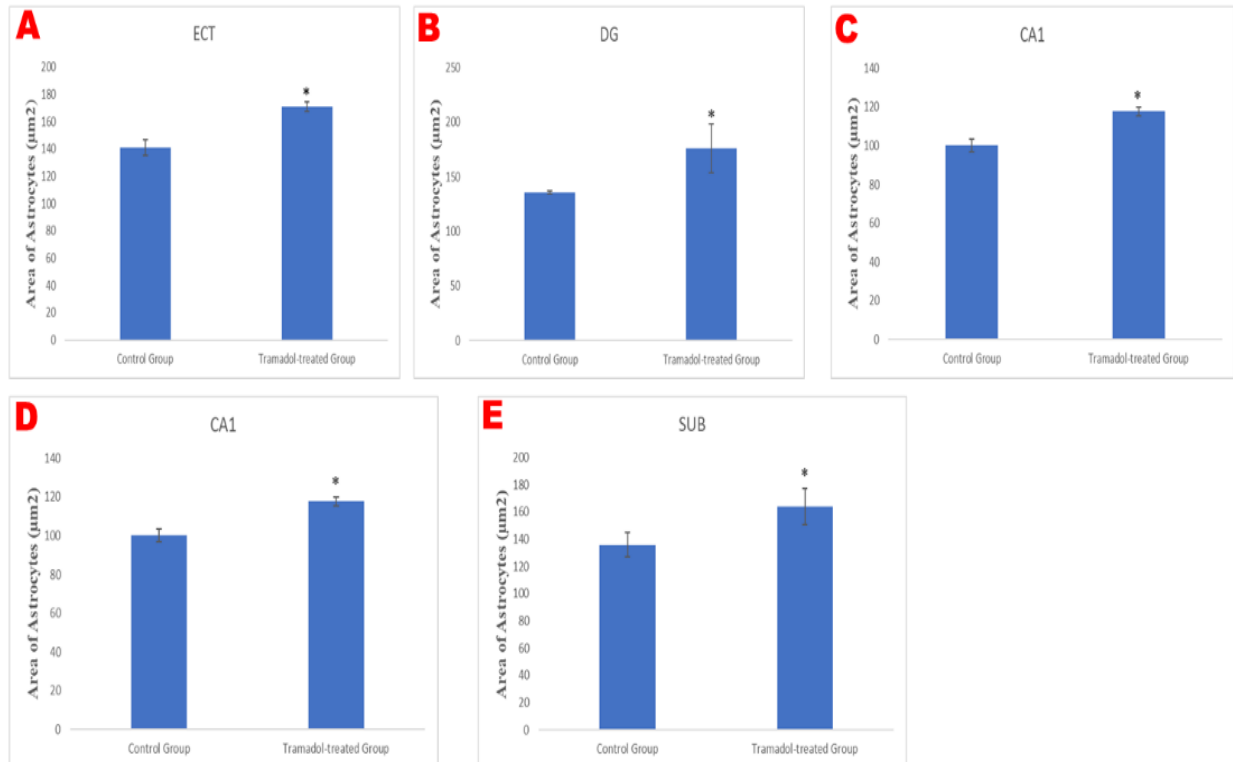


Figure 15: Area of reactive astrocytes of Wistar rats following oral administration of tramadol. n=6; mean ± SEM, student t-test, Tukey post-hoc test, *=p<0.05 when compared to control. Control = 2 ml/kg of distilled water, Tramadol-treated group = 50 mg/kg, ECT = entorhinal cortex, DG = dentate gyrus, CA1 = cornu ammonis, CA3 = cornu amonis, SUB = subiculum (A, B, C, D & E).

DISCUSSION

Tramadol is being used more frequently across the globe since it is thought to have fewer negative effects than other opioids (Zhuo *et al.*, 2012). Because it accelerates neurodegeneration in numerous areas of the brain, tramadol, a synthetic counterpart of codeine can cause a variety of behavioral deficits and histopathological changes. Additionally, when taken orally, it might be swiftly absorbed (Groud & Sablotzki, 2004), and it has the potential to quickly cross the blood-brain barrier, having a variety of impacts on the central nervous system (CNS) (Hosseini-Sharifabad *et al.*, 2016).

The hippocampal formation is a complex structure located in the medial temporal lobe of the brain. It is believed to be involved in memory, spatial navigation, and attention management. In all mammals, the hippocampal formation's neuronal architecture and circuits are remarkably similar (Anderson *et al.*, 2007). One of the parts of the brain that is particularly prone to damage is hippocampal formation. Significant cognitive abnormalities, such as memory impairment and problems with spatial navigation, can result from damage to this region (Smith *et al.*, 2003). As a result, the effects of tramadol on the hippocampal formation's structural components, spatial learning, and memory were investigated.

This study assessed the effect of tramadol treatment on the body weight of rats. There was a significant increase ($p < 0.05$) between the initial and final body weights after 21 days in the control and the tramadol group. No significant difference was observed when the final body weight was compared between the two groups. Mohamed *et al.* (2015), in their study on the effects of tramadol, clonazepam and their combination on the brain mitochondrial complexes, observed a reduction in body weight in groups treated with tramadol. Oyedeji, in a 2020 study, reported a significant reduction in body weight at a later stage during the treatment

period with tramadol (0.71 mg/kg). He suggested in the study that this could result from tramadol increasing the catabolism of lipids in the adipose tissue, which caused the reduction in the weight of the rats at the later stage of treatment. Balogun *et al.* (2020) reported that single-dose treatment of tramadol at 20 mg/kg body weight reduced the amount of food consumed by rats compared to the control group and that the rats exposed to tramadol were low in weight when compared to the control. Additionally, Nielsen *et al.* (2019) reported inhibition of fish foraging and eating habits after exposure to prescription drugs at doses similar to environmental concentrations. In addition, recreational, illicit and prescription drugs such as tramadol, Viagra etc could influence various mental processes leading to some behavioural deficits (Balogun *et al.* 2020). Gould, 2010, wrote that a single dose of some drugs might result in temporary cognitive impairments causing the inability of the person to remember to eat correctly and the possible onset of weight loss. People who abuse drugs may eventually suffer from permanent impairments in brain activity and physical changes that could lead to dramatic weight loss and poor health (Vieira, 2015). Studies have shown that analgesic drugs in the opiate class cause varying degrees of side effects, including drowsiness, nausea, vomiting and constipation. Such side effects can lead to decreased appetite, slowed digestion and weight loss (McCabe *et al.*, 2015). Symptoms of the reported side effects of opiates, particularly nausea and vomiting, can lead to a lack of nutrients and an imbalance of electrolytes, resulting in difficulty maintaining a healthy body weight (Balogun *et al.*, 2020). In this study, there was no significant ($p>0.05$) difference in percentage (%) body weight change when final body weight was compared across the groups. This result agrees with the work of Mohamed and Mahmoud (2019), who observed that administration of 30 and 60 mg/kg body weight of tramadol for eight weeks did not induce significant changes in the body weight of rats when compared with the control group.

This study's result revealed no significant difference in the brain-body weight index (BBWI) of Wistar rats. However, there was a slight decrease in the brain-body weight index (BBWI) of group 2 compared to the control. The effects of the neurotoxicity of tramadol are known, and continuous administration of tramadol resulted in weight loss in rats' brains (Zhuo *et al.* 2012).

Histochemical assessment of the structures of the hippocampal formation using CFV stain in this study, revealed histopathological changes such as karyolysis, cytoplasmic vacuolation, dark neuron, perineural vacuolation, chromatolysis and indistinct staining intensity of the hippocampi in tramadol-treated group. The observed neuronal degeneration associated with the loss of Nissl bodies and reduced staining intensity of the Nissl substances in the tramadol-treated group may be attributed to the detrimental effect of tramadol administration, suggesting that tramadol may be involved in neurodegeneration. Nissl bodies have been shown to decrease as a result of neuronal degeneration (Ekpo *et al.*, 2023). A reduction in the number of Nissl bodies results from damage to axons or neuronal exhaustion brought on by severe or persistent stimulation. Nuclear migration to the periphery of the perikaryon coincides with this change known as chromatolysis, which lowers the RNA level (Takano, 1964). Additionally, poisonous and chemical chemicals have an impact on the Nissl substance, altering its metabolic activity (Davis & Robertson, 1991).

Awadalla and Salah-Eldin (2016) observed alterations in the Nissl substance in the cerebral cortex and the hippocampus, presenting a pale blue colour of Nissl granules at the rims of the cytoplasm of most of the neurons, indicating a decrease in the Nissl substance in their study

on Molecular and histological changes in the cerebral cortex and the lung tissues under the effect of tramadol treatment.

Astrocytes, the most prevalent type of glial cell in the brain, is essential for preserving brain homeostasis. They are engaged in a number of processes, such as recycling neurotransmitters, regulating blood flow, and exchanging nutrients and waste. Additionally, astrocytes are essential for synaptic plasticity and neural signaling (Li *et al.*, 2018). In this study, the microscopic examination of the structures of the hippocampal formation using glial fibrillary acidic protein (GFAP) stain revealed various activation responses of astrocytes in the tramadol-only treated group such as having numerous reactive astrocytes processes; extensive overlapping and interdigitation of astrocytes processes; astrocytes proliferation; astrocytes cell body hypertrophy and thickening of astrocytes processes. In agreement with this research, Adekomi *et al.* (2019) examined the effects of alcohol and tramadol co-treatment on cognitive functions and neuro-inflammatory responses in the medial prefrontal cortex of juvenile male rats. They found that after administration of 60 mg/kg twice daily to young rats for 30 days, they experienced abundant reactive astrocyte processes followed by significant loss of neurons. Barbosa *et al.* (2021) observed increased GFAP expression in the brain cortex upon exposure to the lowest and intermediate opioid doses. In their study, GFAP hippocampal immunoreactivity increased in the juvenile and adult mice treated with 40 mg tramadol/kg/day for one month coupled with astrogliosis. Another study found that giving 50 mg/kg/day of tramadol intraperitoneally for four weeks boosted GFAP expression, as seen by astrocytes' enlarged cell bodies and thickened processes (Motawea *et al.*, 2020). Similarly, Ekpo *et al.* (2023) in their study on *Zingiber officinale* ameliorates tramadol-induced histopathological distortions in CA1 and CA3 of the hippocampus of adult wistar rats observed overexpression of GFAP in the tramadol only treated group when compared to the control.

Numerous researches back up the idea that GFAP overexpression contributes to opioid tolerance and dependence (Ekpo *et al.*, 2023). Therefore, increased GFAP expression in the current study is a sign of glial proliferation and hypertrophy seen in the histopathological examination; these, in turn, are a response to opioid-induced injury, which may change synaptogenesis and neurogenesis, as well as lead to apoptosis and/or necrosis (Hussein *et al.*, 2020).

CONCLUSION

This study's findings demonstrate the negative impacts of tramadol on body weight, brain weight, Nissl substance and astrocytes activation.

ACKNOWLEDGMENTS

The authors wish to acknowledge the Department of Human Anatomy, staff of Histology and Neuroscience Units of Ahmadu Bello University, Zaria for their technical assistance towards the success of this work.

REFERENCES

- Adekomi, D. A., Adegoke, A. A., Olaniyan, O. O., Ogunrinde, A. E., & Ijomone, O. K. (2019). Effects of alcohol and tramadol co-treatment on cognitive functions and neuro-inflammatory responses in the medial prefrontal cortex of juvenile male rats. *Anatomy*, 13(1), 1-12. <https://doi.org/10.21767/0974-7230.100023>
- Akunna, G. G., & Lucyann, C. A. (2023). Nigeria's War Against Drug Abuse: Prevalence, Patterns, Ramifications, Policy and Multisectoral Response, Strategies and Solutions.

- Studies in Social Science & Humanities*, 2(10), 35-55. <https://doi.org/https://doi.org/10.22158/sss.v2n10p35>
- Amber, W. S., Musa, S. A., Sambo, S. J., & Agbon, A. N. (2020). Nephroprotective effect of *Citrus sinensis* L. on mercury-exposed Wistar rats. *Annals of Tropical Pathology*, 11(2), 157. https://doi.org/10.4103/atp.atp_14_20
- Anderson, P., Morris, R., Amaral, D., Bliss, T., & O'Keefe, J. (2007). The hippocampal formation. In P. Anderson, R. Morris, D. Amaral, T. Bliss, & J. O'Keefe (Eds.), *The hippocampus book* (pp. 3). Oxford University Press.
- Awadalla, E. A., & Salah-Eldin, A. E. (2016). Molecular and histological changes in cerebral cortex and lung tissues under the effect of tramadol treatment. *Biomedicine & Pharmacotherapy*, 82, 269-280. <https://doi:10.1016/j.biopha.2016.05.011>
- Balogun, S. K., Osuh, J. I., & Onibokun, O. O. (2020). Effects of separate and combined chronic ingestion of codeine and tramadol on feeding behavior of female albino rats. *Journal of Medical Research and Health Sciences*, 3(7).
- Barbosa, J., Faria, J., Garcez, F., Leal, S., Afonso, L. P., Nascimento, A. V., & Dinis-Oliveira, R. J. (2021). Repeated administration of clinically relevant doses of the prescription opioids tramadol and tapentadol causes lung, cardiac, and brain toxicity in Wistar rats. *Pharmaceuticals*, 14(2), 97. <https://doi.org/10.3390/ph14020097>
- Carson, F. L. (1997). *Histotechnology: A self-instructional text* (2nd ed.). American Society of Clinical Pathologists Press.
- Davis, R. L., & Robertson, D. M. (1991). *Textbook of neuropathology* (2nd ed.). Williams and Wilkins.
- Dayer, P., Desmeules, J., & Collart, L. (1997). The pharmacology of tramadol. *Drugs*, 53, 18-24.
- Dinis-Oliveira, R. J. (2019). Metabolism and metabolomics of opiates: A long way of forensic implications to unravel. *Journal of Forensic and Legal Medicine*, 61, 128-140. <https://doi.org/10.1016/j.jflm.2018.12.002>
- Eichenbaum, H. (2017). Prefrontal-hippocampal interactions in episodic memory. *Nature Reviews Neuroscience*, 18(9), 547-558. <https://doi.org/10.1038/nrn.2017.74>
- Eisch, A. J., Barrot, M., Schad, C. A., Self, D. W., & Nestler, E. J. (2000). Opiates inhibit neurogenesis in the adult rat hippocampus. *Proceedings of the National Academy of Sciences*, 97(13), 7579-7584. <https://doi.org/10.1073/pnas.97.13.7579>
- Ekpo, U. U., Umana, U. E., & Sadeeq, A. A. (2023). Zingiber officinale ameliorates tramadol-induced histopathological distortions in CA1 and CA3 of the hippocampus of adult Wistar rats. *Journal of Neurobehavioural Sciences*, 10(2), 29-40. <https://doi.org/10.5897/JNBS2022.0068>
- Ekpo, U. U., Umana, U. E., Sadeeq, A. A., Shuaib, Y. M., Oderinde, G. P., Dauda, K., & Teryila, G. A. (2023). Zingiber officinale exhibits neuroprotective properties against tramadol-induced spatial memory impairment and histopathological changes. *Nigerian Journal of Neuroscience*, 14(3), 86-95.
- Eluwa, M. A., Ekanem, T. B., Udoh, P. B., Ekong, M. B., Asuquo, O. R., & Akpantah, A. O. (2013). Teratogenic effect of crude ethanolic root bark and leaf extracts of *Rauwolfia vomitoria* (Apocynaceae) on Nissl substances of albino Wistar rat fetuses. *Neuroscience Journal*, 2013, 619405. <https://doi.org/10.1155/2013/619405>
- Fanselow, M. S., & Dong, H. W. (2010). Are the dorsal and ventral hippocampus functionally distinct structures? *Neuron*, 65(1), 7-19. <https://doi.org/10.1016/j.neuron.2009.11.031>
- Gould, T. J. (2010). Addiction and cognition. *Addiction Science & Clinical Practice*, 5(2), 4-14. <https://doi.org/10.1151/ascp10224>
- Grond, S., & Sablotzki, A. (2004). Clinical pharmacology of tramadol. *Clinical pharmacokinetics*, 43(13), 879-923. <https://doi.org/10.2165/00003088-200443130-00004>

- Nielsen, S. V., Frausing, M., Henriksen, P. G., Beedholm, K., & Baatrup, E. (2019). The psychoactive drug escitalopram affects foraging behavior in zebrafish (*Danio rerio*). *Environmental Toxicology and Chemistry*, 38(9), 1902-1910. <https://doi.org/10.1002/etc.4502>
- Oyededeji, K. O. (2020). Effect of Tramadol on Reproductive Parameters in Male Wistar Rats. *International Journal of Pharmaceutical Sciences Review and Research*, 62(2), 1-5. <https://doi.org/10.1016/j.ijpsrr.2020.03.001>
- Schoenbaum, G., Roesch, M. R., & Stalnaker, T. A. (2006). Orbitofrontal cortex, decision-making and drug addiction. *Trends in neurosciences*, 29(2), 116-124. <https://doi.org/10.1016/j.tins.2005.12.006>
- Smith, D. H., Meaney, D. F., & Shull, W. H. (2003). Diffuse axonal injury in head trauma. *Journal of Head Trauma Rehabilitation*, 18(4), 307-316. <https://doi.org/10.1097/00001199-200307000-00001>
- Suvarna, S. K., Layton, C., & Bancroft, J. D. (2019). Stains for Nissl substance: Techniques for staining neurons. In *Bancroft's Theory and Practice of Histological Techniques* (8th ed., pp. 308-309). Elsevier.
- Takano, I. (1964). Electron microscopic studies on retrograde chromatolysis in the hypoglossal nucleus and changes in the hypoglossal nerve, following its severance and ligation. *Okajimas Folia Anatomica Japonica*, 40(1), 1-69.
- Toufique, S. E. I. D. U. (2022). Factors influencing the abuse of tramadol among tricycle (Yeloyelo) drivers in the Tamale metropolis (Doctoral dissertation).
- United Nations Office on Drugs and Crime. (2019). Key findings of UNODC study on tramadol trafficking in West Africa discussed at regional meeting. Retrieved from <https://www.unodc.org/unodc/en/frontpage/2019/July/key-findings-of-unodc-study-on-tramadol-trafficking-in-west-africa-discussed-at-regional-meeting.html>
- Wiffen, P. J., Derry, S., & Moore, R. A. (2017). Tramadol with or without paracetamol (acetaminophen) for cancer pain. *Cochrane Database of Systematic Reviews*, (5).
- Yoshida, Y., Koya, G., Tamayama, K., Kumanishi, T., & Abe, S. (1990). Development of GFAP positive cells and reactive changes associated with cystic lesions in HTX rat brain. *Neurological Surgery*, 30(7), 445-450. <https://doi.org/10.2176/nmc.30.445>
- Zhuo, H. Q., Huang, L., Huang, H. Q., & Cai, Z. (2012). Effects of chronic tramadol exposure on the zebrafish brain: a proteomic study. *Journal of proteomics*, 75(11), 3351-3364. <https://doi.org/10.1016/j.jprot.2012.03.038>